

L-band RFI Measurement and Mitigation at the NSRT Site*

LIU Qi^{1,2†} LIU Ye¹ CHEN Mao-zheng¹ WANG Yue¹ LIU Feng¹
YAN Hao¹ CAO Liang¹ SU Xiao-ming¹

(¹ *Xinjiang Astronomical Observatory, Chinese Academy of Sciences, Urumqi 830011*)

(² *University of Chinese Academy of Sciences, Beijing 100049*)

ABSTRACT Radio environment degrades significantly at Nan Shan 26 m Radio Telescope (NSRT) base due to new and upgraded electrical devices on-site and more establishment of surrounding radio communication services. How do we mitigate them effectively? Firstly, a quasi-real time Radio Frequency Interference (RFI) measurement method is employed for RFI detection and spectral analysis based on the layout for potential on-site interference areas and off-site radio communication services. Our investigation at the frequency bands for pulsar observations (1380–1700 MHz) indicates that transient interferences pose the greatest impact on observations. Then we use a portable RFI measurement system for interferences hunting at the NSRT, and the typical characteristics of interferences are analyzed. Secondly, based on the RFI characteristics, main interference sources in the observation room are shielded with shielding cabinets. The results from our shielding efficiency (SE) measurement and evaluation show that these methods work effectively. Furthermore, we propose a Radio Quiet Zone (RQZ) and the regulations for NSRT to mitigate off-site RFIs.

Key words radio environment, RFI characteristic, RFI mitigation, shielding efficiency

Classified index: P111; **Document code:** A

1 Introduction

The NSRT base, as shown in the Fig. 1, is located at the northern foot of Tianshan Mountain in the center of Eurasian Continent with the longitude and latitude of

Received 2019-04-16, revised version 2019-06-11

*Supported by Chinese Academy of Sciences (CAS) “Light of West China” Program, The National Natural Science Foundation (11973077, 11473061), The Operation, Maintenance and Upgrading Fund for Astronomical Telescopes and Facility Instruments, budgeted from the Ministry of Finance of China (MOF) and administrated by the CAS

[†]liuqi@xao.ac.cn

87°10.67'E and 43°28.27'N, respectively. It is situated at an altitude of 2080 m, and more than 70 km away from Urumqi city. The NSRT is equipped with four cryogenic receivers operating at L, S/X, C, and K bands (see Table 1, in which ST is the System Temperature of the receiver, LCP and RCP are the Left-hand Circular Polarization and Right-hand Circular Polarization, respectively). The unique geographical location makes the telescope to be an important node of Very Long Baseline Interferometry (VLBI) observations for both domestic and international observations. In addition, the NSRT contributes the fundamental research in radio astronomy as well, such as pulsars, molecular lines, and active galactic nuclei.



Fig. 1 The NSRT site

Table 1 Specifications of the receivers on NSRT

Receiver	Center Frequency/MHz	Bandwidth/MHz	Polarization	ST/K
L	1560	320	LCP/RCP	22
S/X	2300/8600	400/800	LCP/RCP	21.5/70
C	4915	370	LCP/RCP	50
K	23100	2200	LCP/RCP	35

Radio environment of NSRT is deteriorated for several reasons as follows. Firstly, the recent upgrades on the NSRT include the installment of various new electronic equipments, such as monitoring and controlling electronics, digital backends, safety equipments, and optical telescopes, which introduce potential on-site RFI sources. The Fig. 2(a) shows the distribution of the on-site potential RFI sources at the NSRT base. However, shield protection and effective equipment management are ignored during this process^[1]. Secondly, the range of frequency occupancy is getting broader with the development of technology. The Fig. 2(b) shows the distribution of off-site potential

RFI sources, which indicates that many transmitters are operating around the NSRT base. Therefore, it is a challenge to identify the RFI sources and their associated signal features for the RFI mitigation.

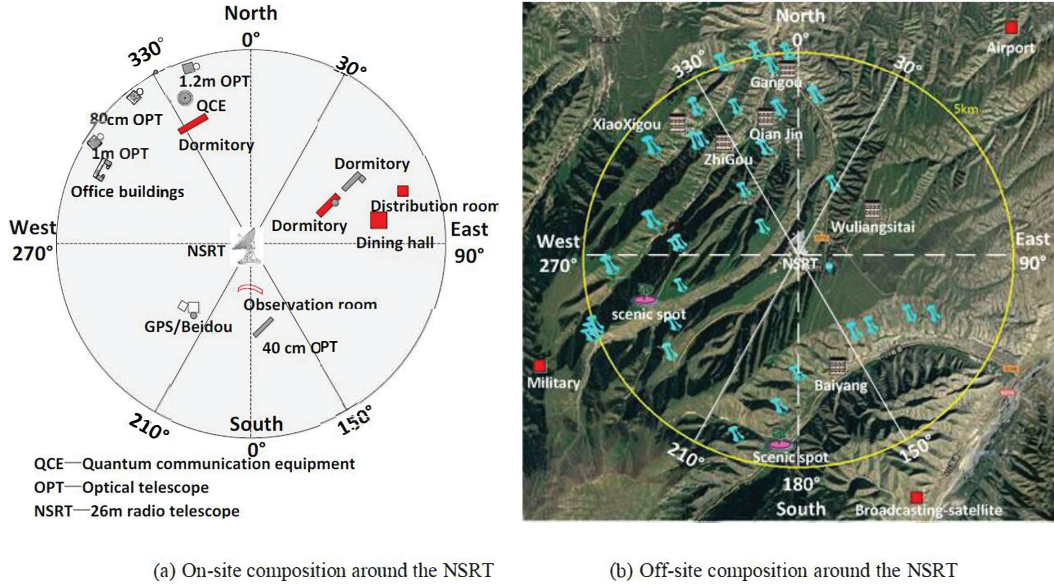


Fig. 2 Overview of the potential on-site (a) RFI sources, about 600 m range around the NSRT, and off-site (b) RFI sources, where a circular region with a radius of 5 km is indicated by the yellow boundary, and the spots in cyan are mobile phone base stations.

2 RFI detection and characteristic analysis

2.1 RFI measurement system

A portable RFI measurement system is employed for this work. Fig. 3 shows the diagram of this system, including a Schwarz-beck 9143 directional antenna, a broadband Low Noise Amplifier (LNA) with maximum gain of 30 dB, a Personal Computer (PC) controlling the R&S FSW13 spectrum analyzer with the General Purpose Interface Bus (GPIB) cable, and a standard noise source with the 24 V Direct Current (VDC) power supply interface. We develop a program on the Visual Studio 2013 platform for the control of spectrum analyzer and data storage. The performance of this system is tested by the Y-factor method^[2] showing in Fig. 4, indicating that the system sensitivity is good enough for strong RFIs detection.

2.1.1 Measurement methods

(1) The RFI detection system is installed on the NSRT at a height close to the feed aperture for both horizontal and vertical polarizations RFI measurements. The RFI levels obtained at this position can be used to analyze the RFI impacting on observations effectively.

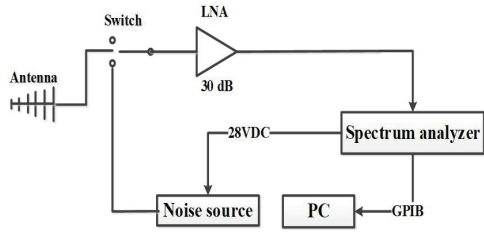


Fig. 3 Diagram of the RFI measurement system

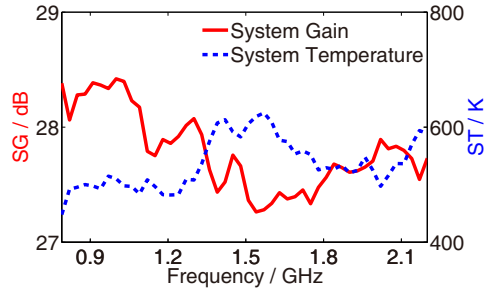


Fig. 4 System Gain (SG) and system noise temperature

(2) Key parameters set for spectrum analyzer are as follows: Resolution Band Width (RBW) = 30 kHz, Video Band Width (VBW) = 300 kHz, we obtain ten points at every RBW, and the sweep time at one RBW is 100 μ s; Sample detector and the average trace mode are applied for the measurement, the average time is set to 200 times to improve the signal-to-noise ratio. From the above parameters, the sweep time for one span can be calculated for testing.

(3) In order to improve the RFI data accuracy, system gain and system noise temperature are measured beforehand. We use the system gain for data calibration; and we can also determine the system reliability according to the system noise temperature.

(4) The 3 dB beam width of the measuring antenna is about 45° , therefore, R-FIs are tested by controlling the NSRT with 45° intervals at a fixed elevation of 10° , which ensures no obstructions impacting on RFI measurement. It is assumed that the northward direction is 0° and the southward direction is 180° .

(5) A quasi-real-time method is used for daytime RFI measurements from UTC (Coordinated Universal Time) +8 (Beijing time) 10:00 to 22:00 with 1.5 h intervals for one polarization^[3], which enables us to analyze the RFI variations against time.

2.1.2 Data processing and analyzing

Data processing: we calculate the average values of every 10 points at each RBW band as the final levels corresponding to the channel frequency.

Data calibration: assuming RFI level at antenna aperture is P , in unit of dBm, which can be calculated according to Eq. (1),

$$P = P_{SA} - G_A - G_S, \quad (1)$$

where P_{SA} is the signal level obtained by the spectrum analyzer, in unit of dBm; G_A is the gain of the testing antenna; G_S is the gain of the RFI measurement system except the testing antenna.

Then P is further converted into field strength E , in unit of $\text{dB}\mu\text{V} \cdot \text{m}^{-1}$, based on

Eq. (2),

$$E = P + AF + 107, \quad (2)$$

where AF is the antenna factor.

Interference signals of the spectra from all directions at one time period are counted. The statistical graph is presented in the Fig. 5, which shows that narrow signals from 180°, 225°, and 270° are greater than those from other directions. Based on the analysis of the distribution of the potential on-site RFI sources as mentioned in the introduction section, most of the RFIs are suspected to come from on-site electronics.

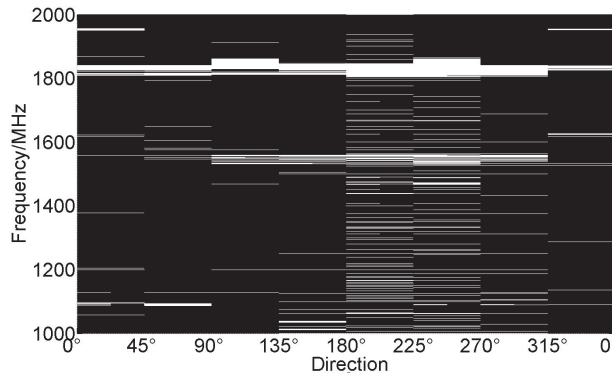


Fig. 5 Statistic of the interference signals from all directions. The black color is the background noise, and the white lines are the signals identified.

The Frequency Channel Occupancies (FCOs) for pulsar observation band (1400–1700 MHz) are counted as well. The bandwidth of each channel in the digital filter-band is 512 kHz, while the RFI frequency resolution is 30 kHz. So during the statistical process, if one 512 kHz bandwidth in radio environment spectra existing in interference signals, it can be seen that this channel is occupied. The FCO is defined as the percentage of channels occupied vs. the total channels in this paper. The FCO of spectra from all directions and time periods are counted, as presented in the Fig. 6^[3]. This statistical graph shows the FCO varies greatly in the same direction, indicating that transient RFI has great impact on observations.

2.1.3 Interference source analysis

In order to verify the RFI sources, measurement steps are as follows: (1) the RFI testing system is installed on the NSRT close to the feed aperture, pointing at the equipment areas (180°). And the measuring antenna is about 30 m away from the equipment areas; then the spectra from both the on-site equipment area and off-site radio environment are tested. (2) The RFI testing system is installed on the top of the most external building at the same height crossing to the equipment areas, pointing to the same direction, as shown in the Fig. 7. Then off-site radio environment can be

measured in the same direction. A comparison of the spectra between the equipment area and off-site radio environment is presented in Fig. 8, indicating that most of the narrow RFIs come from the on-site equipment areas.

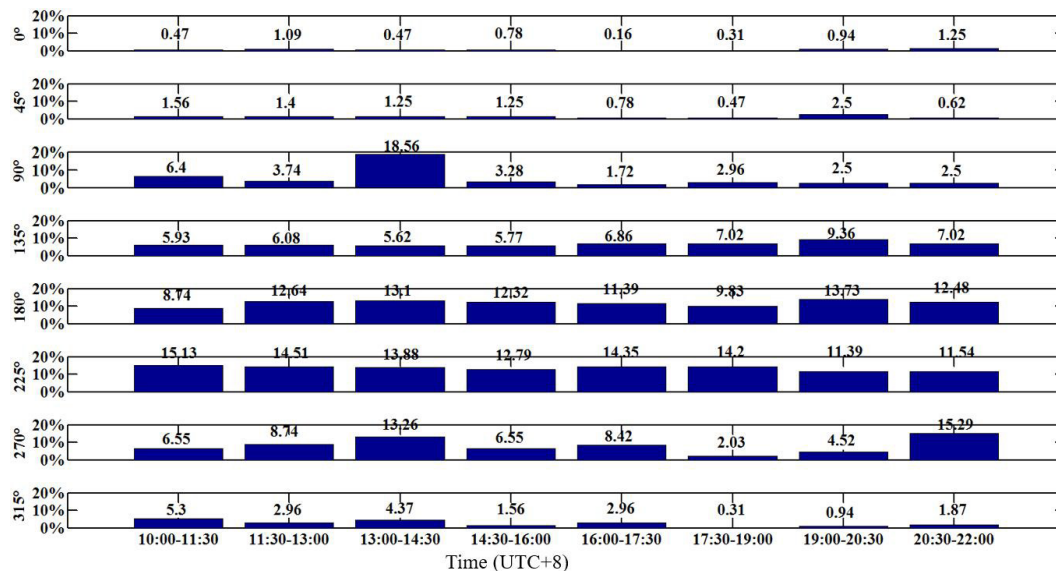


Fig. 6 This plot presents frequency channel occupancy vs. time and direction, the frequency channel occupancy of all spectra is marked on the plot for clearance.

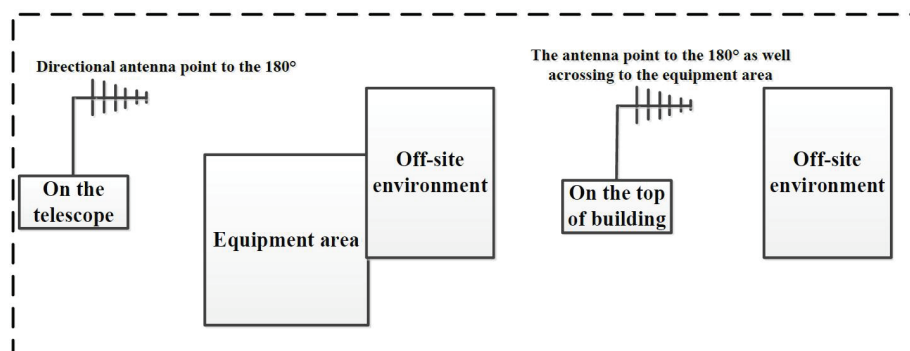


Fig. 7 RFI source verification

Furthermore, the primary RFI sources in equipment areas are tested using a portable on-site RFI measurement system^[4]. The distance for measurement is set to 1 m; the sample detector and average trace mode are employed for radiate emission testing. Measurement results indicate that the primary RFI sources include servos, network equipment, backends, digital switches, industrial computers and so on. Typical RFI sources and their characteristics are presented in Fig. 9, which shows that their emission characteristics are always broadband below 3 GHz; meanwhile emissions from

some digital devices are extremely noisy compared to the environment noise (Fig. 9(b)).

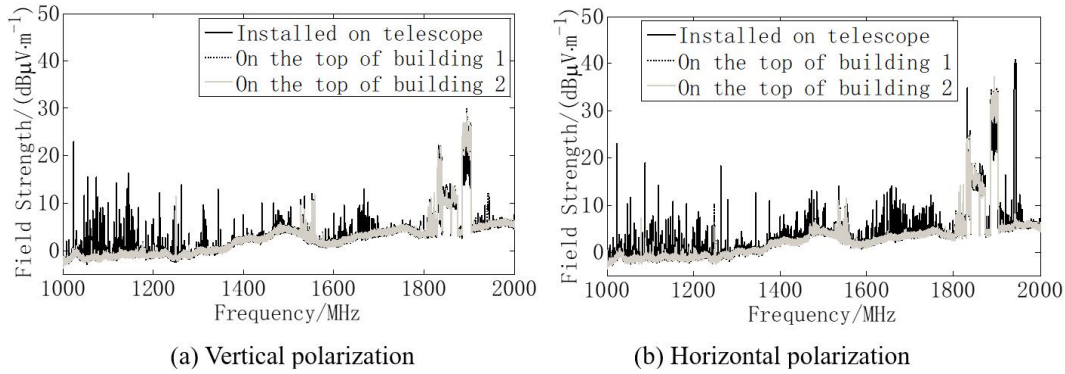


Fig. 8 Two-state measurement spectra between equipment areas and RFI environment in the direction of 180° . (a) and (b) are the vertical and horizontal polarization measured results, respectively. The black line is the spectra tested on the telescope, and the dotted and gray lines are the RFI environment spectra measured on the top of the building.

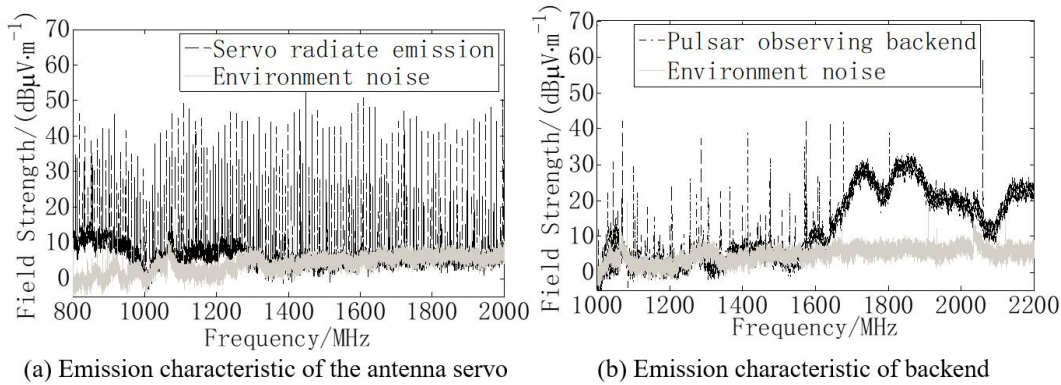


Fig. 9 Radiate emissions for the typical digital equipment, (a) shows the emission characteristic of the antenna servo, (b) presents the emission characteristic of the typical backend, where the gray line is the environment noise tested by shutting down all electrical devices.

2.2 RFI measurements using the NSRT

Due to NSRT is more sensitive than the RFI measurement system, in order to further hunt and analyze the characteristics of RFI signal, the NSRT is employed for RFI detection at L band. The Fig. 10 shows the measurement system links, and the intermediate frequency (IF) spectra from the L-band receiver obtained by the R&S FSW13 spectrum analyzer. For practical testing, the spectra are obtained at 15° intervals in the case of elevation = 10° . The measurements analyzing shows the main interference comes from the off-site radio communication services, such as broadcasting satellite, Global Positioning System (GPS), Global Navigation Satellite System (GLONASS), Inmarsat, cell phone stations, military services, and on-site electronics according to

the International Telecommunication Union (ITU) radio regulations¹ and our on-site interference measurements.

From the detected RFIs and the analyzed results shown above, we select several strong RFI sources for further analysis of their characteristics, especially for the 1440–1495 MHz band, which have great impacts on the pulsar observation.

(1) The extremely strong RFI sources come from the azimuth at 255° , as shown in the Fig. 11, this broadband interference can be identified in the azimuthal direction from 225° to 270° with the NSRT, and the frequency bands are 1460–1480 MHz, 1485–1495 MHz, and 1630–1650 MHz. The interference also makes the L-band receiver saturation when NSRT operating at the azimuthal direction between 255° and 245° , and at the elevation range from 8° to 13° . For this interference, we have sought for its origin several times in the mountains along the direction of 255° . However, we can hardly confirm its source because of the complex terrain. But the azimuthal range that leads to receiver saturation is coded in the pulsar observation software to avoid the strong RFI, the efficiency of pulsar observation is thus increased.

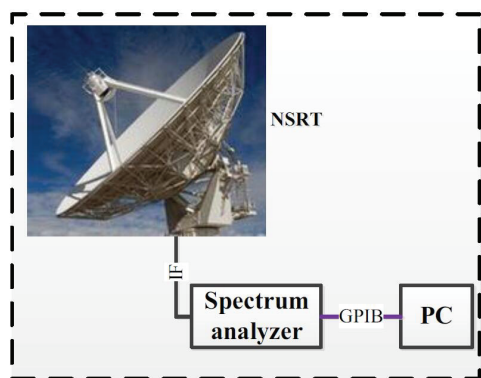


Fig. 10 RFI measurement diagram using the NSRT, the IF signals from L-band receiver were sent to spectrum analyzer.

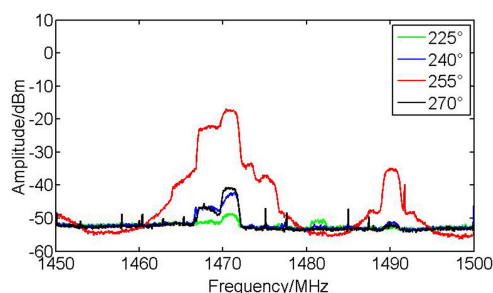


Fig. 11 Strong RFI in the direction of 255°

(2) Another strong RFI sources come from the 155° , which can be identified with NSRT in the azimuthal direction ranging from 130° to 190° , covering from 1467 to 1492 MHz, including five sub-bands (1467–1471 MHz, 1471–1476 MHz, 1476–1479 MHz, 1479–1484 MHz, 1484–1492 MHz), as shown in the Fig. 12. According to the broadcasting-satellite service^[5], this interference comes from satellite digital audio radio uplink service. However, the location of the transmitter could not be determined due to little information provided by local government and the complex terrain factor. Therefore, we should further communicate with the local government for coordinating on this RFI in the future.

¹<http://search.itu.int/history/HistoryDigitalCollectionDocLibrary/1.43.48.en.101.pdf>

(3) When using the NSRT for RFI measurements, we notice that a strong interference appears at the L band between 1400 and 1500 MHz, which does not vary with AZ. Obviously, this interference impacts on observations greatly. From our experience, the interference may come from the telescope itself. In order to search for this RFI source, the portable interference testing system is used to measure the possible equipment area of the telescope. And we find that the RFI source comes from the newly installed IF switching system in the receiver cabinet. When this system is shut down, the interference signal in the L-band spectrum disappears, as shown in the Fig. 13. Now, the IF switching system is turned off during pulsar observations, and we are planning to shield this system in the future.

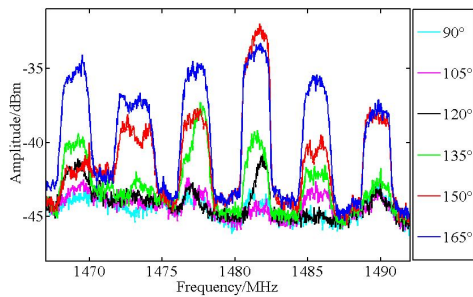


Fig. 12 RFI characteristics of the broadcasting satellite

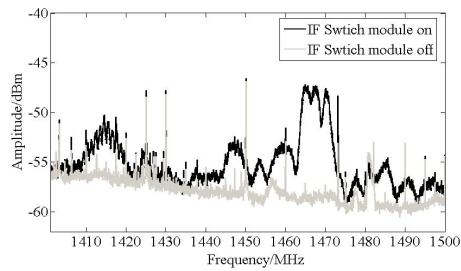


Fig. 13 Spectra of the IF Switch during on and off

(4) Other strong on-site RFI characteristics are presented in the Fig. 14(a), which shows that the emissions can enter the telescope receive system directly. The Fig. 14(a) shows a lot of narrow signals in the pulsar observing band with an interval of 1.25 MHz from 1580 to 1700 MHz in the azimuthal direction of 195°. Based on the RFI characteristics and the measurement results, the interference source is located coming from the newly installed Fast Radio Burst (FRB) backend close to the window in NRST observing room. The Fig. 14(a) indicates that the interference disappeared when the system is shut down. Furthermore we shield this interference source with a shielding cabinet.

In addition, we find that this interference can be detected obviously when NSRT operating at the azimuth between 120° and 270°, and with the Elevation of 10°, as shown in Fig. 14(b). We speculate that this RFI may enter the telescope through the antenna side lobe and the sub-reflector reflections. In order to figure out how the interferences are coupled into the telescope, we need to investigate this issue by further measurement and simulation analysis.

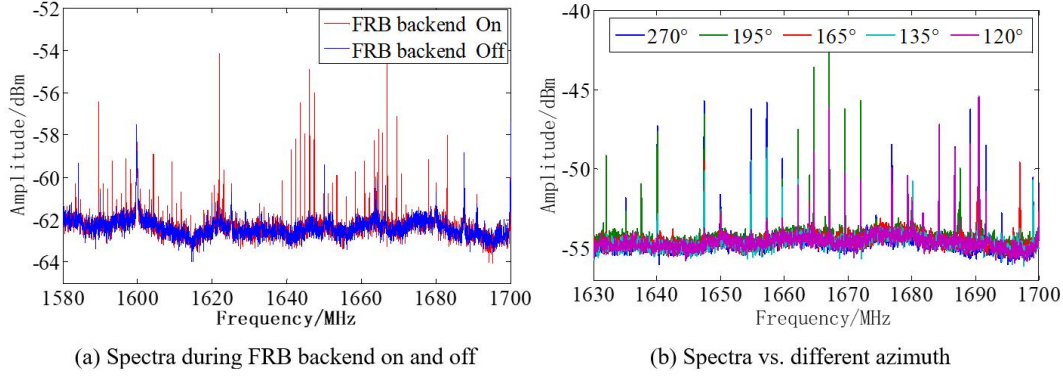


Fig. 14 RFI characteristics of the FRB backend, Fig. 14(a) presents the spectra during FRB backend on and off, Fig. 14(b) shows the spectra vs. different azimuth.

3 RFI mitigation

3.1 On-site RFI mitigation

Based on the detected RFIs and their characteristics at NSRT site, it is not easy to shield all interference sources in a short time. So we are trying to shield the main RFI sources in the NSRT observing room within our funds available. Shielding efficiency requirements for the RFI source analysis are as follows: (1) the RFI mitigation is for pulsar observations, so the shielded frequency band we cared about is 1.4–1.7 GHz. (2) Interference level limit is -175 dBm for the continuum observations at 1.4 GHz^[6]; (3) The maximum radiate emissions of the digital equipment counted is -75 dBm at the L band; (4) the NSRT observing room is about 37 m away from the telescope feed aperture, and the path loss calculated with free-space propagation model is about 64 dB; (5) the antenna gain calculated according to the parabolic antenna gain model is about -5 dBi^[7–9]. The shielding efficiency (SE) S_E requirements can be calculated according to Eq. (3),

$$S_E = TL - G_{\text{sidelobe}} + G_{\text{Loss}} - P_E - U, \quad (3)$$

where S_E is the SE requirements, TL is the interference level limit at feed aperture of telescope, G_{sidelobe} is the antenna gain, G_{Loss} is the path loss from the observing room to telescope, P_E is the measured radiate emission of the equipment, U is measurement uncertainty. By assuming the measurement uncertainty is 6 dB, the largest calculated SE requirement is 37 dB.

We propose a shield scheme for the primary RFI sources (including Intra-Day Variability (IDV), FRB, Digital Filter Bank (DFB), Analog Filter Bank (AFB) backend; time and frequency system; the controlling computers for Antenna Control Unit (ACU), Field System (FS), VLBI system, and others) in the observing room using shielding boxes, as shown in Fig. 15. And we customize the power line and signal cable filters

that installing on interface boards for every cabinet to avoid conducted emission over cables. In addition, in order to realize the network supplying and shield the ethernet devices effectively, the optical fiber links are employed to replace the previously ethernet cables.

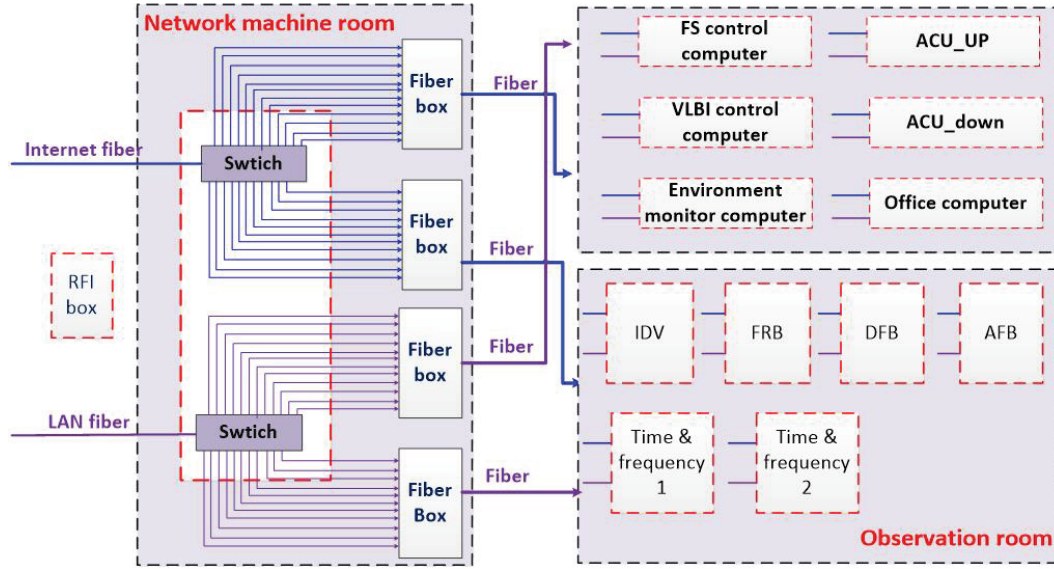


Fig. 15 Shielding schematics using RFI cabinets, the dashed line box represents shielding cabinets, the fibers from the switch to the shielding box for ethernet supply.

In order to verify the effectiveness of electromagnetic shielding enclosures, the SE of the RFI cabinets is measured on-site according to the IEEE standard method^[10], and the SE is calculated on the basis of Eq. (4),

$$S_E = P_1 - P_2, \quad (4)$$

where P_1 is the reference power intensity without the enclosure; P_2 is power intensity with the enclosure in place, in unit of dBm.

SE measurement results for the doors and interface boards of the shielding cabinets are presented in Fig. 16. The figure indicates that the SE of the shielding box are more than 60 dB below 3 GHz, so testing results meet the shield requirements.

In order to further verify the effectiveness of this shielding work, radiate emissions of the typical interference are tested between the shielding doors opening and closing statuses when the interference sources are installed in the shielding cabinets. And the differences of spectral statuses are presented in the Fig. 17, which shows that the emissions can be mitigated more than 40 dB between 1000–2000 MHz. Due to the radiate emission levels of RFI sources and the sensitivity of RFI measurement system, this verification method is not the standard SE measurement method as well, which

leads to the SE measurement differences between Fig. 16 and Fig. 17. However, all measurement results indicate that the SE is enough based on the requirement evaluation analysis above.

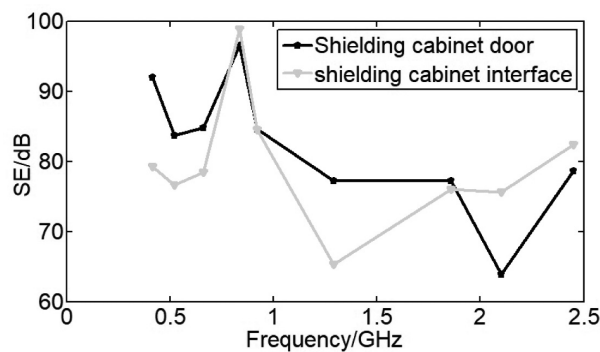


Fig. 16 SE measured for shielding cabinet at the cable connected status

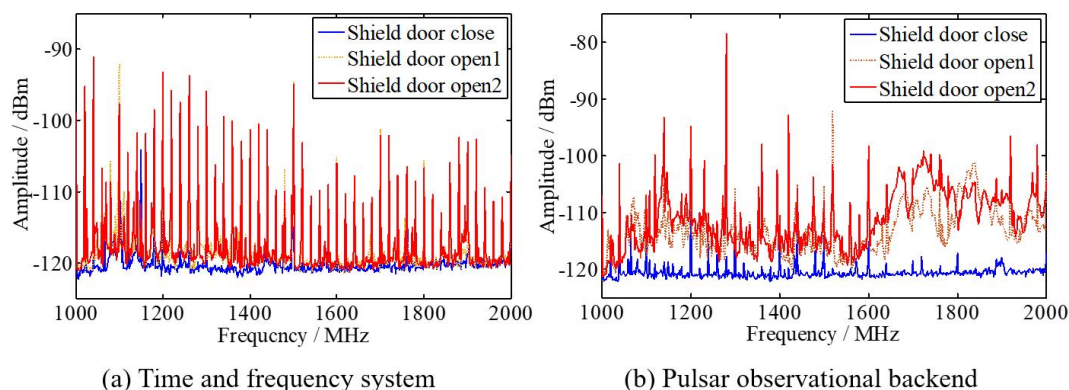


Fig. 17 Spectra measured when the shield door is open vs. close. Fig. 17(a) shows the shielding cabinet of the time and frequency system testing results; Fig. 17(b) presents the shielding cabinet of pulsar observational backend.

The antenna servo and control system are strong RFI sources, as shown in Fig. 9(a). However, it is a challenge for us to shield them due to its high power and various cables coming into and out of the servo modules. If we shield them using traditional method (shield and filter), the cost will be extremely high. From the analysis above, we are planning to move the servo system from the NSRT observing room to the basement under the telescope such that its radiate emissions can be mitigated by the reinforced concrete of the basement. After this work, we make an evaluation for the impact of the servo emission on observations, the results are as follows: (1) the interference level limit for pulsar observation of the NSRT is -175 dBm; (2) the propagation loss from servo to the L-band receiver feed aperture is 58 dB; (3) the antenna gain calculated according to parabolic antenna gain model is about -8 dBi^[8]; (4) The maximum RFI

levels at the L band is -95 dBm; (5) Reinforced concrete SE measurement result is more than 20 dB, and the SE measurement for servo cabinet door is about 10 dB. From the calculated and measured results above, the servo emissions propagating to the feed aperture of the NSRT is -191 dBm, which is obviously below the pulsar observation limit, indicating that this RFI protection work is effective.

3.2 Off-site RFI protection

In recent years, increasing number of new radio communication facilities were constructed in the off-site area around the NSRT, especially the mobile base stations, which have great impacts on pulsar observations. Therefore, a circular region of Radio Quiet Zone (RQZ) with a radius of 10 km is proposed as shown in the Fig. 18(a). The off-site RFI protection is conducted with the following requirements: (1) No new transmitter is allowed in the circular region within a radius of 5 km from the NSRT; (2) All operating transmitters within the view of the telescope, and located within a radius of 5 km need to be removed; (3) No new transmitter within the view of the telescope is allowed in the range of 5 to 10 km region; (4) Local government should provide accurate information for all transmitters available in the RQZ for the interference regulation in the future.

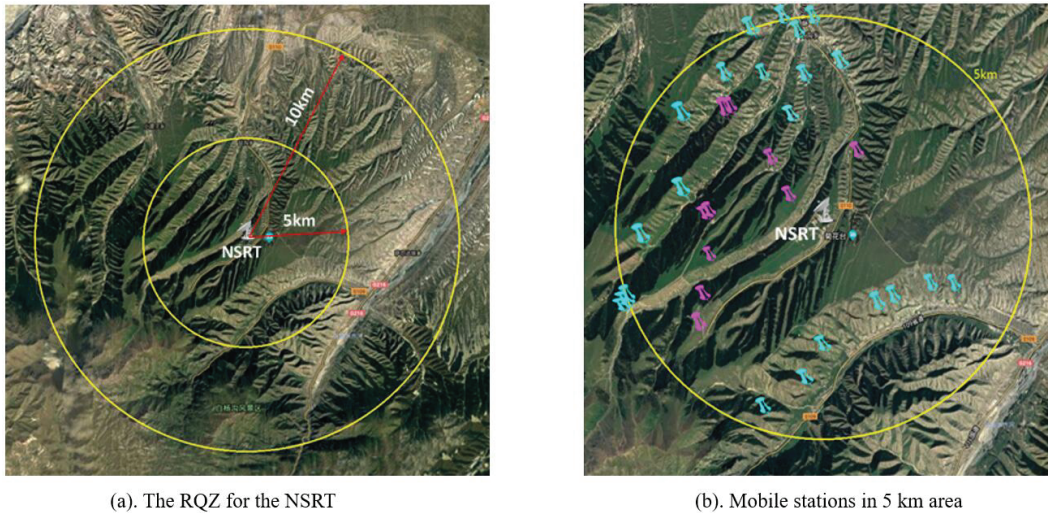


Fig. 18 The RQZ for the NSRT is shown in map (a), and mobile stations are marked with signs in blue and purple in map (b). The purple ones will be removed.

We are proposing the above requirements to the local governments, and to ensure that we can negotiate with the authorities and the regulatory department responsible for the radio transmitters regulation. Meanwhile, the mobile stations within the view of the telescope, and located within a radius of 5 km, as shown in Fig. 18(b), should be removed first.

4 Conclusions

A portable RFI measurement system and the NSRT are employed for our RFI environment testing and interference hunting; meanwhile we analyze the characteristics of RFIs. The conclusions are as follows: (1) Transient RFIs have great impacts on observations; (2) Both on-site and off-site RFIs can enter the receiver from different azimuths through side lobe and sub-reflector reflections; (3) Despite the AZ and EL changes, RFIs can always be coupled into the receiver system of telescope, which greatly impact on the observations.

Additionally, we are trying to shield the primary RFI sources in the NSRT observing room. The results from the SE measurement and emission evaluation indicate that these mitigation works are effective.

Although we do some work for the RFI measurements and mitigation, many problems remain to be solved in the future. So our work plans are as follows: (1) It is extremely important to enforce on-site electrical equipment management policy so that the RFIs from new electronics can be controlled effectively; (2) There are still many RFI sources at the NSRT site, so the mitigation work will continue; (3) It is necessary for us to figure out the coupling principle between telescope and interference for the further RFI hunting and mitigating; (4) Off-site RFI coordination with the local government is proceeding; (5) A real-time RFI detection system will be developed for further transient interferences analysis.

Reference

- [1] Zhang Q T, Liu Q, Sun Z W, et al. Science Technology and Engineering, 2016, 16: 191
- [2] Liu Q, Wang K, Wang Y, et al. AR&T, 2014, 11: 218
- [3] Liu Q, Wang N, Wang Y, et al. Chinese Journal of Radio Science, 2017, 32: 718
- [4] Liu Q, Liu F, Liu Y, et al. Progress in Astronomy, 2016, Supplement.: 124
- [5] Hovstad P, Sung L. International Journal of Satellite Communications and Networking, 2005, 23: 91
- [6] ITU. Protection criteria used for radio astronomical measurement: Recommendation ITU-R RA.769-2. ITU, 2003
- [7] Liu Q, Chen M Z, Li Y, et al. AR&T, 2015, 12: 292
- [8] Liu Q, Liu Y, Wang N, et al. Proceedings of 2016 Radio Frequency Interference. Socorro: IEEE, 2017: 55-58
- [9] ITU. Space research earth station and radio astronomy reference antenna radiation pattern for use in interference calculation, including coordination procedures, for frequencies less than 30GHz: Report ITU-R SA.509-3. ITU, 2013
- [10] IEEE. IEEE Standard method for measuring the effectiveness of electromagnetic shielding enclosures: IEEE Std 299-2006. IEEE, 2007